Properties of Single-Domain, Pseudo-Single-Domain, and Multidomain Magnetite

SHAUL LEVI[1]

Department of Geology and Geophysics, University of Minnesota, Minneapolis, Minnesota 55455

RONALD T. MERRILL

Geophysics Program and Oceanography Department, University of Washington, Seattle, Washington 98195

Despite the influence that paleomagnetism has exerted on the earth sciences, our understanding of thermal remanent magnetization (TRM), which is one of the primary sources of paleomagnetic information, is at best fragmentary and incomplete. In this paper we report on experiments studying TRM properties of magnetites whose particle sizes vary from single domain (SD) to pseudo single domain (PSD) to multidomain (MD). TRM stability has been measured by using alternating field (af) demagnetization, hot af demagnetization, low-temperature treatments, thermal demagnetization, and storage tests. Low-temperature treatments are a great aid in helping to determine whether a sample's TRM is carried primarily by SD, PSD, or MD magnetite particles. Thermal demagnetization is relatively insensitive for predicting particle sizes, while af demagnetization remains the best method for reducing the MD contribution to the remanence. Theoretical considerations indicate that the thickness of a domain wall should initially increase with temperature until a critical value is reached, beyond which the thickness decreases. This result is useful in the interpretation of the hot af demagnetization experiments of MD particles whose median destructive alternating field increases with temperature up to some maximum value before decreasing, while the median destructive field of SD and PSD particles decreases monotonically with temperature. Characteristics of the Lowrie-Fuller test (Lowrie and Fuller, 1971) for equidimensional 0.2-μm-sized particles indicate that a critical TRM-inducing field h_c exists, where $0.10 < h_c < 0.49$ Oe; SD-like behavior is exhibited when the inducing field is greater than h_c, and MD behavior is exhibited for fields less than h_c. This suggests that the critical sizes for transitions of domain structure depend on the intensity of the inducing field. It is argued that the presence of an external field and, similarly, blocking at high temperatures increase the effective size region of SD/PSD remanence and that remanence might be blocked in grains with a nonequilibrium domain configuration. Estimates of critical sizes for transitions between SD, PSD, and MD behavior depend on several factors including grain shape, temperature, type of remanence given to the sample, mineralogy, and intensity of the field used to induce the remanence.

INTRODUCTION

Néel's [1949] theory of thermal remanent magnetization (TRM) of noninteracting single-domain (SD) particles has been successful in explaining many (though not all) of the observed properties of natural remanent magnetization (NRM) in baked clays and igneous rocks. However, optical observations of magnetic minerals of igneous rocks, which exhibit stable NRM, show that the particle sizes are usually much larger than expected critical diameters of the SD to multidomain (MD) transition of these minerals. This led to the development of MD theories [*Néel*, 1955; *Everitt*, 1962*b*; *Stacey*, 1958; *Schmidt*, 1973] and to theories of SD-behaving regions within a MD matrix [*Verhoogen*, 1959; *Ozima and Ozima*, 1965]. For particles larger than the SD critical size but smaller than the size of 'truly' MD behaving particles (17 μm for magnetite, according to *Stacey* [1962]), *Stacey* [1962, 1963] developed a theory for pseudo-single-domain (PSD) particles for which the TRM is inversely proportional to the particle volumes and changes in remanence occur by discrete Barkhausen jumps of the domain walls. Further developments of PSD theories have been made by *Dunlop et al.* [1974] and *Stacey and Banerjee* [1974, pp. 60–62, 110–114]. In this paper the term PSD is used to refer to magnetite particles whose sizes and magnetic properties are intermediate between truly SD and truly MD particles. Extensive optical and electron microscope studies of the magnetic constituents of igneous rock in conjunction with their magnetic properties [*Evans et al.*, 1968; *Strangway et al.*, 1968; *Hargraves and Young*, 1969; *Evans and Wayman*, 1970] have shown that in many rocks a significant fraction of the remanence carriers are submicron in size. It is now recognized that carriers of TRM in rocks span the gamut from SD to PSD to MD.

Because the construction of viable theories of TRM requires the knowledge of various magnetic parameters, a considerable amount of experimental work has been undertaken in recent years to delineate various magnetic properties as a function of particle sizes and domain states [*Everitt*, 1961, 1962*a*; *Parry*, 1965; *Dunlop and West*, 1969; *Lowrie and Fuller*, 1971; *Dunlop*, 1969, 1972, 1973; *Rahman et al.*, 1973; *Johnson et al.*, 1975; *Bailey*, 1975; *Day et al.*, 1976]. Although it is essential to have the experimental data to test the various TRM theories, it is often unclear how to relate these data to a particular theory. For example, which experimental coercivity does one substitute for the microscopic coercivity in *Néel*'s [1949] SD theory? Even more uncertain is the choice of experimental coercivity that should be used in *Néel*'s [1955] equations for MD remanence. How are the parameters which are obtained from saturation hysteresis loops related to remanence acquired in weak fields? The above uncertainties and complexities are particularly real for TRM, because all the magnetic parameters are temperature dependent.

Many studies in recent years have tried to develop experimental methods to distinguish between remanence carried by SD, PSD, and MD particles. *Parry* [1965], *Rahman et al.*

[1] Now at School of Oceanography, Oregon State University, Corvallis, Oregon 97331.

Paper number 7B0724.
0148-0227/78/017B-0724$03.00

[1973], and *Day et al.* [1976] have used hysteresis properties, whereas *Lowrie and Fuller* [1971], *Dunlop et al.* [1973], *Johnson et al.* [1975], and *Bailey and Dunlop* [1975] have used the characteristics of alternating field (af) demagnetization curves. Clearly, the answer to the question of what is the predominant size of the magnetic carriers in a particular rock (SD, PSD, or MD) must be sought in the context of a particular remanence, because it is not in general true that different types of remanence activate the same distribution of magnetic particles. (Sometimes anhysteretic remanent magnetization (ARM) can be used to model TRM, insofar as stability properties are concerned, as has been shown by *Levi and Merrill* [1976].)

The success of the paleomagnetic method depends on the supposition that a particular rock acquires its remanent magnetism (RM) parallel to the ambient field at the time of its formation and that the rock's RM is stable with respect to geologic time. Although TRM has been subject to studies for over half a century, much remains unknown about which parameters are dominant during the blocking of TRM for different-sized particles, which parameters control the stability of TRM, and how they vary with temperature. It is imperative for the continuing refinement of the paleomagnetic method that we improve our understanding of how RM is acquired and of the different physical mechanisms which control its stability and might cause it to change.

In this paper we report on our TRM studies using particles whose sizes vary from SD to PSD to MD. Magnetite (Fe_3O_4) is used for reasons of experimental convenience and because magnetite is a remanence carrier of many igneous rocks. We try to gain a better understanding of TRM blocking and its stability, to determine the parameters which control them, and to see how they vary with temperature, external fields, and particle sizes. We also seek means for distinguishing between TRM carried by SD, PSD, and MD particles.

Sample Description

This paper deals with magnetites that vary widely in size and origin. It is crucial to most of the following to describe these samples well, so that others can duplicate the work here or possibly explain differences between our results and those of other workers.

Synthetic magnetites were received from the Columbian Carbon Company (CCC), Pfizer Company (BK-5099), and Toda Industries. In addition, we synthesized our own magnetite according to a recipe by *Elmore* [1938]. All the synthetic magnetites have a foreign cation impurity content of less than 1%. It has been well known since the work of *Gallagher et al.* [1968] that magnetites prepared at room temperature by precipitation in an aqueous solution are usually oxidized to some degree or other. Regions of γ Fe_2O_3 may exist, and solid solution between Fe_3O_4 and γ Fe_2O_3 may be present, and possibly even regions of iron hydroxides (see the review by *Merrill* [1975]). The extent of this oxidation is usually variable but sometimes quite large. Since γ Fe_2O_3 and Fe_3O_4 are well known to exhibit different magnetic properties, a lack of reproducibility of experiments between different laboratories is to be expected if precautions are not taken.

All our synthetic samples were heated above 600°C for 6.5 hours in a slightly reducing environment: a residual nitrogen atmosphere at 10^{-1} torr, with carbon as a reducing agent. This heating reduced the γ Fe_2O_3 to stoichiometric magnetite, as is indicated by the increase in J_S and by the increase in the lattice parameter to that of Fe_3O_4 (8.39 ± 0.01 Å). In addition, the temperature treatment at 600°C also altered the internal strain through annealing. A decrease in line broadening of X ray diffraction peaks of the heated synthetic magnetites was observed, consistent with either grain growth, strain release, or improved stoichiometry [*Gallagher et al.*, 1968] (acting together or individually, these causes would have the same effect on line broadening).

Comparison of electron microscope pictures before and after heating indicates that no measurable differences in size or shape have occurred for the CCC and Pfizer magnetites, but a substantial increase in size due to heating was exhibited by the *Elmore* [1938] magnetite. Figure 1 gives a summary of the size distributions for the synthetic magnetite samples after heating. A total of 232 particles in two photographs were measured for the CCC magnetite (samples 6 and 7), 111 particles in two photographs for the Pfizer magnetite (sample 5), and 249 particles in three photographs for the 'Elmore' magnetite (samples 8 and 9). Although photographs were also taken of the Toda magnetite, which indicated that it is very acicular, it was difficult to measure both length and width of many of the particles from the photographs. Because our crude size data are consistent with those reported by Toda Industries, we use the Toda Industry figure of 0.35 μm × 0.04 μm (approximate axial ratio of 8:1) for the mean particle dimensions.

Table 1 describes some of the effects of heating on the bulk magnetic properties of the synthetic magnetite powders. In all cases, J_S was the same or increased after heating, a result expected if γ Fe_2O_3 conversion to Fe_3O_4 occurs. The relatively large effect of heating on the magnetic properties of the Elmore samples is believed to be due, at least in part, to grain growth of superparamagnetic grains into the stable single-domain size range. This is supported by the large increase (after heating) of J_{RS}/J_S, H_C, and H_{CR} and the large decrease of H_{CR}/H_C. The effect of heating on the Toda and Pfizer magnetites appears negligible, while the effects of heating on the CCC magnetite are probably caused by the reduction of γ Fe_2O_3 and/or annealing. Regardless of the cause we see that the effects of heating vary significantly between samples.

In addition to the synthetic magnetites, four large magnetite crystals, samples MSC-0 ≡ 0, MSC-1 ≡ 1, MSC-2, and MSC-3, were used. Electron microprobe analyses [*Johnson and Merrill*, 1972] of a chip from one of these samples indicated that the magnetite contained less than 0.03 wt % of V, Cr, Mn, Ni, and Mg and had a Ti content of less than 0.05% and an Al content of less than 0.23%. J_S measurements, good to ±2 emu/g, are consistent with the 92.5-emu/g value expected for stoichiometric magnetite. Curie temperatures (good to ±10°C) measured in fields between 500 and 800 Oe to accentuate the Curie point are 580°C, as expected for pure magnetite. X ray diffraction results [*Johnson and Merrill*, 1972] are also consistent with the stoichiometric magnetite interpretation. However, recently, *Hoblitt and Larson* [1975] made detailed scanning electron microscope studies on a chip from one of these crystals and found small nonmagnetic inclusions that appear to be Fe-Al silicates. Although the inclusions are numerous, the total volume of these impurities is clearly small, as is indicated by the above measurements. They probably have a minor effect, if any, on the magnetic measurements reported in this paper. In addition, all the natural magnetite crystals have undergone deformational twinning.

MSC-2 was manually ground and mechanically sieved. Particle fractions were initially separated on the basis of sieves that bracketed them. Electron microscope pictures showed that the median particle sizes of the ground powders are always substantially smaller than the apertures of the smaller

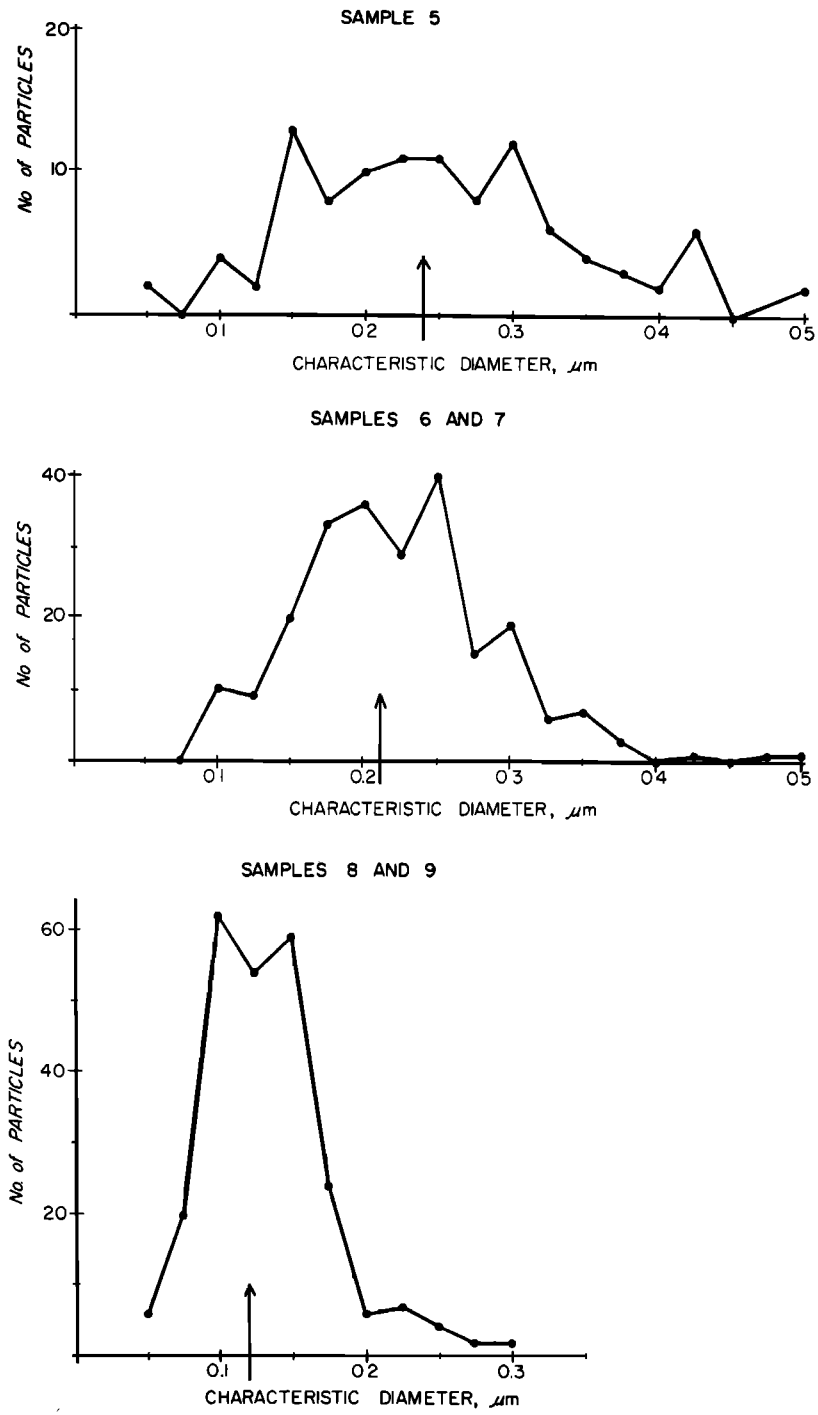

Fig. 1. Particle size distributions of the heated synthetic magnetite powders obtained from electron micrographs. The arrows indicate the distributions' median particle diameters. (Top) Sample 5, Pfizer BK-5099 magnetite powder; $\langle d \rangle = 0.24$ μm; $d < 0.9$ μm. (Middle) Samples 6 and 7, Columbian Carbon Company magnetite powder; $\langle d \rangle = 0.21$ μm; $d < 0.5$ μm. (Bottom) Samples 8 and 9; Elmore magnetite powder; $\langle d \rangle = 0.12$ μm; $d < 0.3$ μm.

bracketing sieve; however, the larger bracketing sieve does establish an upper limit to the particles present. The samples were dispersed in an alumina matrix to be described in detail shortly. Figure 2 illustrates some of the problems involved in characterizing these samples; particles are quite irregular in size, shape, and distribution, and many small particles typically adhere to the larger ones. Considerable effort was made to obtain mean sizes for these samples, as is described elsewhere by *Levi* [1974]. Table 2 summarizes the shape and size data of heated synthetic and natural magnetite particles. Meaningful values of the standard deviations of the median diameters can only be assigned to sample 4 and to the equidimensional synthetic powders (BK-5099, CCC, and Elmore magnetite powders), and they are listed in Table 2.

The magnetite powders were dispersed in an alumina matrix (Alcoa's high-purity alumina powder, A-16) bonded by Alcoa's calcium aluminate cement (Ca-25). The powders were diluted in the matrix to less than 1 wt %, the maximum concentration being less than 4 wt % for sample 3, because of its low J_{RS}/J_S ratio. The mixtures of magnetite and matrix

TABLE 1. The Effect of Heating on the Bulk Magnetic Properties of the Synthetic Magnetite Powders

Magnetite Powder	T_C ±10°C	$H_C(T_R)$ ±<3 Oe		$H_{CR}(T_R)$ ±<7 Oe		$H_{CR}/H_C\|_{T_R}$ ±<0.10		$J_{RS}/J_S\|_{T_R}$ ±0.005	
		Unheated	Heated	Unheated	Heated	Unheated	Heated	Unheated	Heated
Pfizer BK-5099	565	98	100	270	278	2.76	2.78	0.103	0.103
CCC	570	148	105	400	279	2.70	2.66	0.144	0.121
Elmore	575	26.5	112	175	315	6.60	2.81	0.004	0.116
Toda MRM-B-450	591	440	438	600	582	1.36	1.33	0.440	0.448

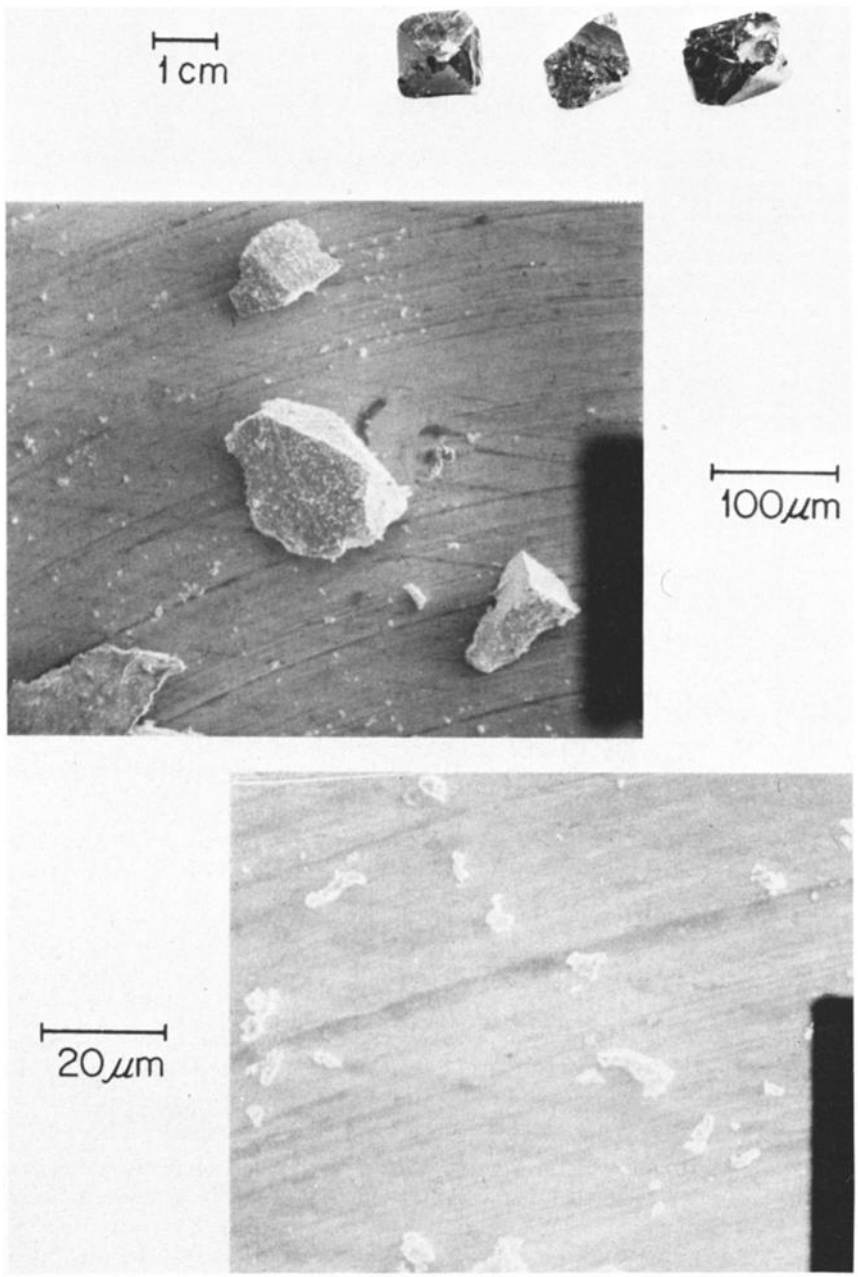

Fig. 2. (Top) Photograph (×1) of the large magnetite crystals resting on one of their respective (111) surfaces. From left to right: MSC-0, MSC-1, and MSC-3. MSC-0 and MSC-1 are identified as samples 0 and 1, respectively, in Table 3. (Middle) Electron microscope picture (×200) of magnetite powder 2, corresponding to sample 2. These particles were retained between 44-μm and 105-μm sieves. Note the large variation in particle sizes. (Bottom) Electron microscope picture (×1000) focusing on some of the smaller particles of the middle photograph.

were sieved through a 250-μm sieve to break down clumps of the matrix and of the magnetite to improve the samples' homogeneity. Samples were molded into cylinders 24 mm in diameter whose height is about 22 mm. Sample volume is usually between 9 and 10 cm^3, and the samples weigh between 15 and 19 g. Samples 6, 6A, 6B, and 6C are different samples prepared in an identical manner from the same batch of CCC magnetite. Sample 7 also contains CCC magnetite and differs from sample 6 only in having approximately 1 order of magnitude greater concentration of magnetite particles. Samples 8 and 9 were prepared identically from the same batch of Elmore magnetite.

Initial experiments with the matrix material suggested that it was nonmagnetic. However, later it was discovered that the material is capable of acquiring a weak TRM. The weak field TRM of a blank sample containing only alumina and calcium aluminate is roughly 1 order of magnitude less than a TRM for the next most feebly magnetized sample (see Table 3, column 2). Extensive experiments described elsewhere [*Levi*, 1974] indicate that the magnetic impurity is probably fine grain magnetite (blocking temperatures of less than 580°C), which is probably produced by the reduction of α Fe_2O_3 impurities when they are heated in a reducing environment. For the sake of comparison the 'blank' was always run along with our other samples in the experiments and is labeled sample 10. The data show that the matrix does not seem to affect the magnetite particles that it hosts beyond the effects of concentration of its own magnetite particles. Other workers may encounter similar problems with alternative matrices when careful analyses are undertaken. The final sample used in this paper comes from the Olby basalt flow in France, which is known to contain SD and/or PSD magnetite [*Whitney et al.*, 1971].

After the samples were prepared, they were slowly heated to 650°C for 6 hours and then given repeated TRM's in the same slightly reducing atmosphere described earlier until the TRM was reproducible to within 2 or 3%.

Equipment and Experimental Procedures

A Schoenstedt slow spinner magnetometer was used for all measurements of remanence. Alternating field demagnetization experiments were conducted by using a four-axis tumbler system in a null-field environment. Thermal demagnetization and low-temperature runs were conducted in a nonmagnetic space ($\pm 50\ \gamma$, equivalently, ± 50 nT). A low-temperature cycle or treatment refers to the process of cooling a sample in a nonmagnetic space below magnetite's isotropic point near 130°K and reheating the sample in the nonmagnetic space to room temperature, where the remaining remanence is measured [*Ozima et al.*, 1964; *Merrill*, 1970]. High-field magnetization versus temperature (J versus T) runs and the determinations of the bulk magnetic properties were conducted on a Princeton Applied Research vibrating sample magnetometer. Unless it is otherwise stated, heating runs were conducted in a vacuum of the order of 10^{-1} torr, with purified nitrogen as the residual gas. A large solenoid was constructed to fit around the nonmagnetic furnace and to connect directly to the inductrol of our af demagnetization unit. This solenoid was then placed inside the nonmagnetic space to allow us to conduct uniaxial hot af demagnetization experiments. Because remanent magnetizations were given in the laboratory to magnetically isotropic samples, the uniaxial af demagnetization at room temperature was found to be essentially identical to af demagnetization in our tumbler system providing, of course, the remanent magnetization was aligned along the axis of the solenoid.

TABLE 2*a*. Physical Description of Heated Natural Magnetites

Sample/ Powder Number	Sieve Size, μm	$\langle d \rangle$	d_{max}, μm	Predominant Shape
MSC-0 ≡ 0		6.378 g		euhedral crystal
MSC-1 ≡ 1		3.569 g		crystal chip
MSC-2		~3 g		crystal chip, flat
MSC-3		9.583 g		euhedral crystal
2	$44 < d < 105$	2.7 μm	150	irregular
3	$d \lesssim 44$	1.5 μm	50	irregular
4	$d < 44$	$0.31 \pm 0.2\ \mu$m	2	regular polygons

Stability of Magnetic Samples

Magnetic stability is usually measured in paleomagnetic studies by one or more of the following techniques: af demagnetization, thermal demagnetization, low-temperature treatment, or storage tests. *McElhinny* [1973, pp. 89–107] gives a brief description of these techniques. Table 3 summarizes the stability versus grain size for our magnetite samples for each of these procedures. The largest changes in stability with respect to thermal demagnetization occur between samples 0 and 2, while the largest changes in stability with respect to af demagnetization and low-temperature cycles occur between samples 1 and 4. As multidomain grains of magnetite are argued not to have coercivities greater than 100 or 200 Oe [*Soffel*, 1971], samples numbered 4 and higher presumably carry TRM in predominately PSD or SD magnetite.

This interpretation is consistent with results from low-temperature treatments. In this regard we note that if the theory of *Kobayashi and Fuller* [1968] is correct, then PSD grains should behave similarly to SD grains during a low-temperature treatment, and the loss of remanence resulting from a low-temperature treatment essentially should be restricted to MD grains [*Kobayashi et al.*, 1965; *Merrill*, 1970]. An examination of the Kobayashi-Fuller theory indicates that the apparent lack of a loss of remanence in SD particles after low-temperature treatment results when shape anisotropy is dominant in pinning the remanence across the isotropic point near 130°K. However, for some nearly equally dimensional magnetite grains whose microscopic coercivity is a result of both shape anisotropy and magnetocrystalline anisotropy, there is some magnetic rotation across the 130°K transition (at which the sum of the magnetocrystalline anisotropy constants changes sign). Therefore no loss is expected for samples containing SD/PSD acicular magnetite, but a slight loss is expected for SD/PSD samples containing more or less equally dimensional magnetite. This expectation is consistent with the data of Table 3, which gives results for each of three successive low-temperature cycles. Essentially no loss is observed for the acicular magnetite, sample 11, while a slight loss is observed for the more equally dimensional submicron magnetite samples. The largest change in the amount lost from a low-temperature treatment occurs between samples 3 and 4. This suggests that the MD contribution to the TRM of sample 3 is substantially greater than it is to the TRM of sample 4.

These results are consistent with J_{RS}/J_S values of the submicron-sized magnetite samples, which have ratios that vary from 0.10 to 0.44 (Table 1). The largest ratio was found for the SD particles with large shape anisotropy. This ratio is smaller

TABLE 2*b*. Physical Description of Heated Synthetic Magnetites

Magnetite Powder	Sample	$\langle d \rangle$, μm	d_{max}, μm	Predominant Particle Shape
Pfizer BK-5099	5	0.24 ± 0.1	0.9	regular polygon; cubes→ spheres
CCC	6, 6A, 6B, 6C, 7	0.21 ± 0.06	0.5	regular polygon; cubes→ spheres
Elmore	8, 9	0.12 ± 0.04	0.3	regular polygon; cubes→ spheres
Toda MRM-B-450	11	0.35×0.04	1.2×0.13	acicular; axial ratio, 8:1

than 0.5 (expected for an assemblage of randomly oriented SD particles), as would be expected if any MD, PSD, or superparamagnetic particles are present. *Davis and Evans* [1976] have shown that magnetic interactions can also cause a reduction in J_{RS}/J_S, the effect being greatest for the most SD behaving samples. Typical J_{RS}/J_S values for samples of larger grain sizes are 1 or 2 orders of magnitude smaller.

A storage test is not usually considered a demagnetization procedure but rather an indication of viscous effects that, presumably, preferentially affect MD grains. The results of the storage tests (Table 3) are more difficult to interpret in a precise manner but appear to be consistent with the interpretations made from the af demagnetization and low-temperature results.

If one expected higher 'stability' with decrease in grain size for the samples in Table 3, then the numbers ranging from 0 to 11 in parentheses in the last four columns, which indicate the samples' relative stability, should progressively increase downward in each column. Of the demagnetization procedures, thermal demagnetization appears to be the least effective in selectively removing TRM in MD grains. The low-temperature treatments are the most correlatable with changes in particle size. Low-temperature treatments detect the presence of MD grains through a loss of remanence during cooling

TABLE 3. TRM Properties of Heated Magnetite Samples

Sample	Mean TRM of Sample, emu/g (h = 0.47 Oe)	$H_{1/2}$, Oe	$\langle T_B \rangle$, °C	Low-Temperature Cycles	Spontaneous Decay
0	0.75×10^{-3}	12 ± 4 (0)	300 ± 40 (0)	0.136 0.110 0.106 (1)	0.926 ± 0.013 (1)
1	1.63×10^{-3}	17 ± 2 (1)	380 ± 80 (1)	−0.091 −0.092 −0.101 (0)	0.924 ± 0.012 (0)
2	1.45×10^{-4}	77 ± 5 (2)	475 ± 15 (5)	0.590 0.465 0.476 (2)	0.938 ± 0.002 (2)
3	1.32×10^{-3}	138 ± 10 (3)	493 ± 10 (7)	0.593 0.521 0.497 (3)	0.970 ± 0.005 (5)
4	0.573×10^{-3}	380 ± 15 (9)	444 ± 10 (4)	0.936 0.889 0.822 (4)	0.990 ± 0.002 (6)
5	1.78×10^{-3}	351 ± 15 (7)	492 ± 10 (6)	0.945 0.935 0.929 (5)	0.992 ± 0.002 (7)
6	0.729×10^{-3}	338 ± 15 (6)	507 ± 10 (9)	0.976 0.951 0.945 (7)	0.995 ± 0.004 (9)
7	7.68×10^{-3}	360 ± 15 (8)	508 ± 10 (10)	0.965 0.961 0.955 (8)	0.998 ± 0.002 (10)
8	0.707×10^{-3}	295 ± 15 (4)	400 ± 15 (2)	0.990 0.971 0.965 (10)	0.967 ± 0.002 (4)
9	0.657×10^{-3}	300 ± 15 (5)	418 ± 10 (3)	0.986 0.910 0.907 (6)	0.958 ± 0.002 (3)
10	0.158×10^{-4}	430 ± 20 (10)	503 ± 10 (8)	0.982 0.974 0.960 (9)	0.994 ± 0.012 (8)
11	1.95×10^{-3}	571 ± 20 (11)	519 ± 10 (11)	1.003 0.995 0.994 (11)	0.998 ± 0.002 (11)

The numbers ranging from 0 to 11 in parentheses in the last four columns indicate the relative stability of the samples. These numbers in the 'Low-Temperature Cycles' column apply to all three values for each sample.

and a partial recovery on heating. However, because some part of MD remanence always remains and because the low-temperature treatment preferentially affects grains whose remanence is held by magnetocrystalline anisotropy, af demagnetization is actually more effective in removing the TRM of MD grains [*Merrill*, 1970].

Contrary to the intuition of many paleomagnetists, there is no clear-cut correlation indicated in Table 3 between $H_{1/2}$ and T_B. The lack of a one-to-one relationship between $H_{1/2}$ and T_B can be illustrated by the theory of single-domain grains. The relaxation time for an ensemble of noninteracting identical single-domain grains of uniaxial anisotropy and in zero external field [*Néel*, 1949] is

$$\tau_{\pm} = \frac{1}{f} \exp\left(\frac{VJ_S H_{ci}}{2kT}\right) \tag{1}$$

where V is volume, k is Boltzmann's constant, T is temperature, and f is the frequency parameter which can be approximated by a constant. At blocking,

$$\left(\frac{VJ_S H_{ci}}{2kT}\right)_{\text{blocking}} = \ln(\tau f)_{\text{blocking}} = C \tag{2}$$

where C is the blocking constant. For a given value of the blocking temperature (and therefore a given value of J_S), (2) can be satisfied by a family of values of V and H_{ci}. Therefore one should not expect a one-to-one relationship between H_{ci} and T_B or between τ and T_B.

An important question concerns the accuracy, as contrasted with precision, of the measurements in Table 3. Of particular importance is the degree to which a given measurement is reproducible in another laboratory when a different magnetite sample of presumably 'identical' properties is used. In this regard we stress again that it is important to make comparisons of properties only for samples that have been stabilized by heating in a controlled atmosphere.

The accuracy is partially reflected by considering samples 6 and 7, which come from the same batch of synthetic magnetite. Sample 7 roughly contains 10 times the volume of magnetite as does sample 6. Because higher packing density of the magnetic mineral is known to reduce the coercivity, the larger value of $H_{1/2}$ for sample 7 than that for sample 6 is a reflection of accuracy and not of packing density. Although the accuracy in this case is barely within the limits of the quoted precision, one would, in general, expect much larger differences to occur in the apparent magnetic properties of seemingly identical magnetites when the measurements are made in different laboratories, especially when the magnetites are synthesized by using different techniques and when different equipment is used in the measurements. Therefore one must be cautious about making too much of small numerical differences in Table 3 and in interpreting similar experiments done in other laboratories.

The Stability of Remanence and Its Temperature Dependence

Introduction

The stability of remanence with time, a property that usually can be best described by referring to the relaxation time τ, is probably the most important magnetic property to paleomagnetists. Although many simplifying assumptions were made by *Néel* [1949], he has derived a relationship (equation (1)) between τ and the intrinsic coercivity H_{ci} that appears to work reasonably well for SD grains. The problem is more complicated for MD grains. In MD grains, H_{ci} is usually associated with the field required to move a domain wall over a particular energy barrier. Although a relationship similar to that of SD particles may be applicable to the relaxation of a single domain wall, it is doubtful that such a relationship is applicable to a MD particle that contains many walls, because of magnetic interaction between different domains. In particular, the stability of MD grains is well known to decrease with increase in the mean particle volume (all other factors constant), in contrast to SD grains, for which the stability increases with mean grain size (equation (1)). Nevertheless, all other factors being equal, one does expect that even in MD grains an increase in H_{ci} is directly related to an increase in stability. At present the problem is even more complicated for PSD grains, primarily because there is no agreement on the magnetic configuration of such grains.

One does not directly measure H_{ci} (although H_{ci} is sometimes calculated from measurements of particle shapes and volumes and knowledge of the predominant magnetic anisotropies). Instead, one measures some other 'coercivity' such as H_C, H_{CR}, or $H_{1/2}$, from which one tries to infer the relaxation time and to construct theories for the origin of remanence in SD, PSD, and MD grains.

The temperature dependence of H_C and H_{CR} has been used to assess how magnetic anisotropy and domain structures influence the magnetic stability [*Rathenau*, 1953; *Morrish and Watt*, 1958; *Dunlop*, 1969]. In this section we report on our measurements of af demagnetization at different temperatures of TRM's in MD, PSD, and SD particles between T_R and T_B to study which magnetic parameters influence the stability and acquisition of TRM and how they depend on the particles' magnetic state. For the PSD particles we compare the temperature dependence of $H_{1/2}$ with that of H_C and H_{CR}.

Experimental Results

Hot af demagnetization experiments were conducted with four single crystals of magnetite (Table 2), an Olby flow sample which contains SD grains, and samples 6B and 6C which contain PSD particles (mean diameter equals 0.21 μm). We consider first the results for the MD grains. After TRM was induced, the samples were thermally demagnetized at the elevated temperature, where they were subsequently af demagnetized. The temperature values are thought to be known to ± 10°C, and the values of $H_{1/2}$ to $\pm 5\%$. The remanences were always measured at room temperature, and the demagnetization curves at each temperature were obtained by normalizing the remanence with respect to the magnetization remaining after the thermal demagnetization step. For the MD crystals the TRM was induced in an external field of 9.1 Oe, because for 0.5-Oe TRM, $H_{1/2}$ was only 20 Oe at room temperature. The results are shown in Figure 3. Three of the samples display a broad maximum between 200° and 400°C. For the fourth sample the curve for $H_{1/2}$ is essentially flat to 400°C. *Rathenau* [1953] also observed a single maximum in the coercivity versus temperature curve for MD particles of Ba ferrite when they were heated from 78°K to their Curie point near 530°K.

Very different behavior from that of the MD grains was observed for samples containing SD grains (Figure 4) and PSD grains (Figure 5). The TRM's in the SD and PSD samples were produced in a 0.5-Oe field, which is greater than the 'critical field' of these PSD magnetite particles (see the section on the effects of the external field on critical sizes for a discussion of the critical field). Therefore the similarity of the $H_{1/2}$ versus T curves for these samples is not surprising. As is expected, the relative stability decreases with temperature. The

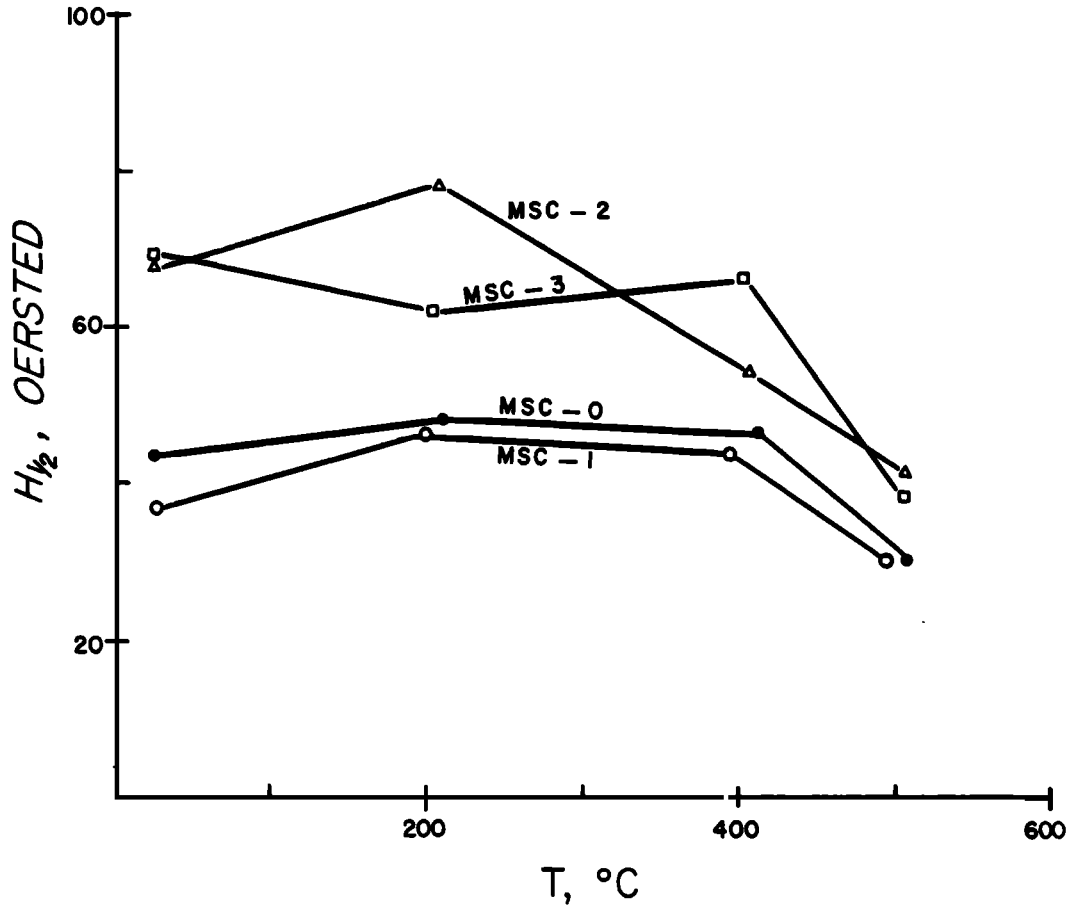

Fig. 3. $H_{1/2}$ (peak oersted) versus temperature plot of the large crystals of magnetite. The curves either are flat up to about 400°C (MSC-3) or display a broad maximum between T_R and 400°C. Note the relatively large scatter in the $H_{1/2}$ values of the different samples.

temperature dependence of $H_{1/2}$ can be approximated reasonably well by a line. The experiments at 500°C were repeated to test the reproducibility of the results (see Figures 4–6). When the lines for $H_{1/2}$ of the different samples are extended to intersect the temperature axes, values close to, or slightly above, the Curie temperature are obtained. Because these values appear too high, we conclude that the stability, as measured by $H_{1/2}$, decreases linearly up to near the blocking temperatures, above which a more rapid decay occurs.

Since many theoretical studies utilize relationships between saturation magnetization and coercivity, it is important to measure these parameters. We felt that this would be particularly interesting for the CCC magnetite particles, whose mean diameters are close to 0.21 μm (samples 6, 6A, 6B, 6C, and 7) because such particles are usually considered to be PSD.

The experiments were performed with undiluted and diluted (roughly to 1.5 wt %) magnetite powder with essentially the same results. This suggests that packing is not a very important variable in these experiments and this particular powder. Figure 6 shows the temperature dependence of J_S, H_C, and H_{CR} normalized to their values at T_R for both diluted and undiluted powders. The measurements were made with our vibrating sample magnetometer; runs were made at low pressures ($\sim 10^{-1}$ torr), with nitrogen the residual gas. J-T runs for these magnetites were found to be reversible under these conditions. For comparison, Figure 6 also shows $H_{1/2}$ (normalized to their values at T_R) versus T curves for samples 6B and 6C. To a reasonably good approximation the data of Figure 6 satisfy the following relationships:

$$H_C \propto H_{CR} \propto J_S^{3/2} \qquad H_{1/2} \propto J_S^{5/2}$$

The different temperature dependences expressed by these proportionalities reflect, in part, the fact that $H_{1/2}$ refers to a TRM, while H_C and H_{CR} involve a saturation isothermal remanent magnetization. It is interesting to note that $H_{1/2}$ decays more rapidly than H_C and H_{CR}.

Ideal SD particles are magnetized to saturation, and their net magnetic moment is equal to VJ_S. However, for particles for which $J_{RS}/J_S < 0.5$, the net magnetic moment is less than VJ_S, and J_S is no longer the appropriate parameter to represent the particles' net magnetic moment. Although it might not be the ideal parameter, it seems that J_{RS} is a better representation than J_S for the particles' mean magnetic moment.

For this reason in Figure 7*a*, H_C and H_{CR} normalized with respect to their T_R values are plotted versus J_{RS} normalized to its room temperature value for both diluted and undiluted CCC powder. All the data are linear to a rather good approximation, and the following relationship is maintained:

$$\frac{H_{CR}(T)}{H_{CR}(T_R)} \simeq \frac{H_C(T)}{H_C(T_R)} \simeq \frac{J_{RS}(T)}{J_{RS}(T_R)} \tag{3}$$

That is, both length and width of the hysteresis loop shrink at the same rate with increasing temperature. In Figure 7*b* we see that

$$\frac{H_{1/2}(T)}{H_{1/2}(T_R)} \simeq \left[\frac{J_{RS}(T)}{J_{RS}(T_R)}\right]^{3/2 \to 4/2} \tag{4}$$

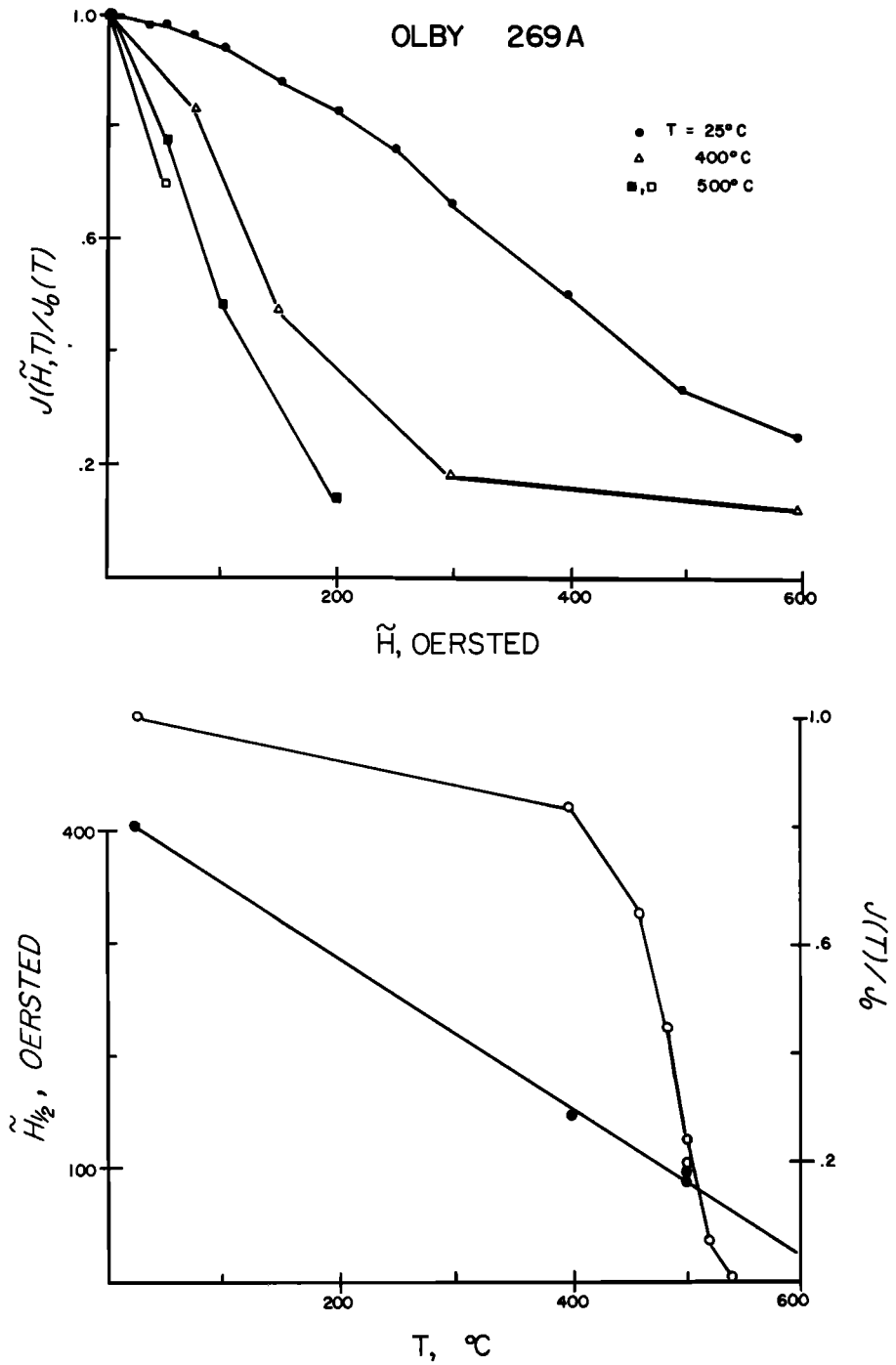

Fig. 4. (Top) Normalized af demagnetization curves at elevated temperatures of 0.49-Oe TRM of basalt sample Olby 269A, whose magnetic carriers are single-domain magnetite particles. The remanence is measured at T_R; the initial points represent the remanence after thermal demagnetization at the temperatures where the af demagnetization was subsequently performed. The demagnetization curves become monotonically 'softer' with increasing temperature. (Bottom) Solid circles (left ordinate) represent the $H_{1/2}$ versus temperature curve; $H_{1/2}$ decreases linearly with increasing temperature. Open circles (right ordinate) represent the sample's normalized thermal demagnetization curve.

where the $H_{1/2}$ data are identical to the $H_{1/2}$ data of Figure 6 and the J_{RS} versus T data were obtained separately, simultaneously with the other hysteresis parameters of Figure 6 (H_C, H_{CR}, and J_S). (Since two independent J_{RS} versus T determinations were made corresponding to both diluted and undiluted powders and because differences in the J_{RS} values are thought not to be related to the dilution of the magnetite powder, with each $H_{1/2}$ determination of Figure 7*b* there are associated two J_{RS} values. Near 500°C the J_{RS} values for the diluted and undiluted powders are indistinguishable; however, at that temperature, two $H_{1/2}$ determinations were made for each sample.)

When H_C/J_{RS} and H_{CR}/J_{RS} data from Figure 7*a* are plotted versus temperature, horizontal lines are obtained (parallel to the temperature axis) for both diluted and undiluted powders. These results show that H_C and H_{CR} are linearly proportional to J_{RS} between T_R and T_C; this suggests that in this temperature range, shape anisotropy is dominant in determining H_C

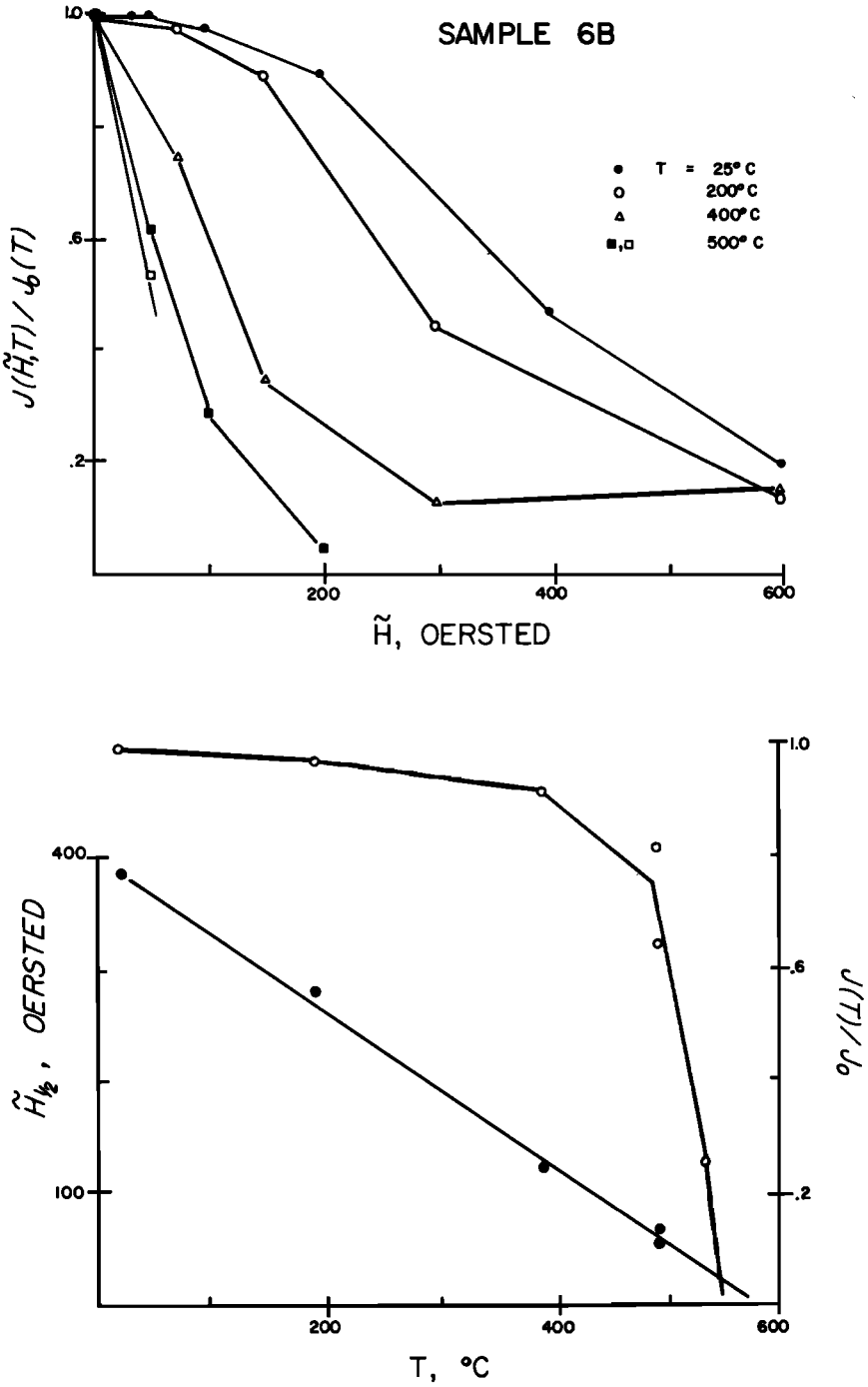

Fig. 5. (Top) Normalized af demagnetization curves at elevated temperatures of 0.49-Oe TRM of sample 6B, whose magnetite carriers are synthetic equidimensional magnetite particles with a mean diameter of 0.21 μm. The remanence is measured at T_R; the initial points represent the remanence after thermal demagnetization at the temperatures where af demagnetization was subsequently performed. The demagnetization curves become monotonically less stable with increasing temperature. (Bottom) Solid circles (left ordinate) represent the $H_{1/2}$ versus temperature curve; $H_{1/2}$ decreases linearly with increasing temperature. Open circles (right ordinate) represent the sample's normalized thermal demagnetization curve.

and H_{CR}. (Significant contributions of magnetocrystalline or magnetostrictive anisotropy would result in a more rapid rate of decay with temperature of H_C and H_{CR}.) In addition, these data do not support the presence of a significant contribution due to thermal fluctuation [*Dunlop and Bina*, 1977] until, possibly, just below T_C, unless thermal fluctuations are also linearly proportional to J_{RS}. Shape anisotropy is also the chief contributor to $H_{1/2}$, but in this case there are also contributions from other anisotropies. These conclusions are consistent with our earlier discussions suggesting that shape anisotropy largely determines the stability of these particles, which results in only a slight loss of remanence after a low-temperature cycle.

There is an inherent ambiguity in measuring H_C and H_{CR} versus temperature, because the ensemble of particles contributing to H_C and H_{CR} changes with temperature as some particles become superparamagnetic. This ambiguity can be

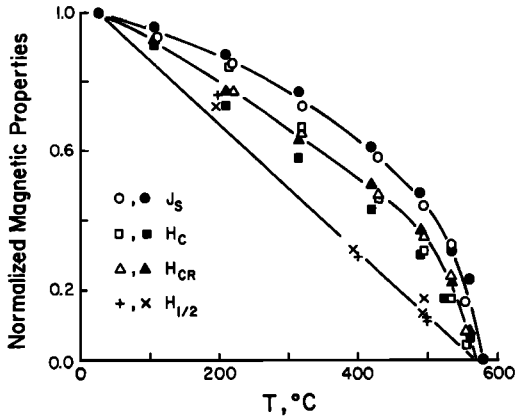

Fig. 6. Hysteresis parameters as a function of temperature for Columbian Carbon Company magnetite powder whose equidimensional particles have a mean diameter of 0.21 μm. Solid symbols represent the undiluted powder, and open symbols represent powder diluted to a concentration of about 1.5 wt %. Circles represent the normalized J_S versus T dependence. Squares represent the normalized H_C versus T dependence. Triangles represent the normalized H_{CR} versus T dependence. Crosses (sample 6B) and pluses (sample 6C) represent the normalized $H_{1/2}$ versus T dependence.

avoided in the $H_{1/2}$ versus T experiment by producing a partial TRM whose temperature interval is above the peak temperature to be used for af demagnetization.

Changes in Domain Wall Thickness With Temperature

At first glance the initial rise observed for $H_{1/2}$ with temperature in MD grains seems puzzling, since all the anisotropy energies that one associates with coercivity in magnetite appear to decrease monotonically with temperature (above room temperature). Because shape anisotropy for SD particles depends linearly on J_S, it decreases with increasing temperature. *Fletcher* [1971] has shown that the magnetocrystalline anisotropy energy for magnetite, as expressed by the magnetocrystalline anisotropy constants K_1 and K_2, decreases with temperature above T_R, where T_R refers to room temperature. This decrease can be expressed in terms of J_S [*Fletcher*, 1971]:

$$\frac{K_1(T)}{K_1(T_R)} = \left[\frac{J_S(T)}{J_S(T_R)}\right]^8 \tag{5}$$

Although K_2 is less well known, it probably also decreases rapidly with temperature [*Morrish*, 1965, p. 321]. Hereafter, K will be used to represent an average magnetocrystalline anisotropy constant. In addition, the magnetostriction anisotropy energy appears to decrease with temperature, as is shown by *Klapel and Shive* [1974].

We will show in the next section that a possible explanation for our observations involves the change in dimension of a domain wall with temperature. The usual treatment of domain walls given in textbooks [e.g., *Cullity*, 1972, p. 290] predicts that the domain wall thickness increases with temperature. These treatments are oversimplified, because they incorrectly treat the temperature dependence of the exchange parameter A and because they neglect to treat the shape anisotropy of the domain wall. *Amar* [1957, 1958] has pointed out that domain walls can possess a significant shape anisotropy that must be considered in many calculations. We will show that the width of a typical domain wall in MD magnetite increases with temperature until a size is reached at which the magnetostatic self-energy of the domain wall dominates the magnetocrystalline anisotropy energy. The width of the domain wall decreases with further increase in temperature. In addition, we will provide reasonable estimates for the temperature dependence of the exchange parameter A. Such estimates are valuable for a wide variety of theoretical calculations.

The exchange parameter A is given by [*Chikazumi*, 1964, p. 273]

$$A = CJ_E J_S^2 \tag{6}$$

where C is a constant with respect to temperature and J_E is the exchange 'constant' that is directly related to electron overlap. The electron overlap of both $3d$ and $4s$ electron orbitals changes with increased temperature, because of thermal expansion and because of increased thermal vibrations. Although we cannot accurately predict the temperature dependence of J_E for magnetite, we can place limits on J_E.

We note that eventually, J_E must decrease with temperature, because at the melting temperature, long-range order disappears, atomic mobility greatly increases, and the electron overlap is substantially lower. Therefore, a reasonable upper limit for J_E is to assume that J_E is constant, independent of temperature. To establish a lower limit for J_E, we note that J_E

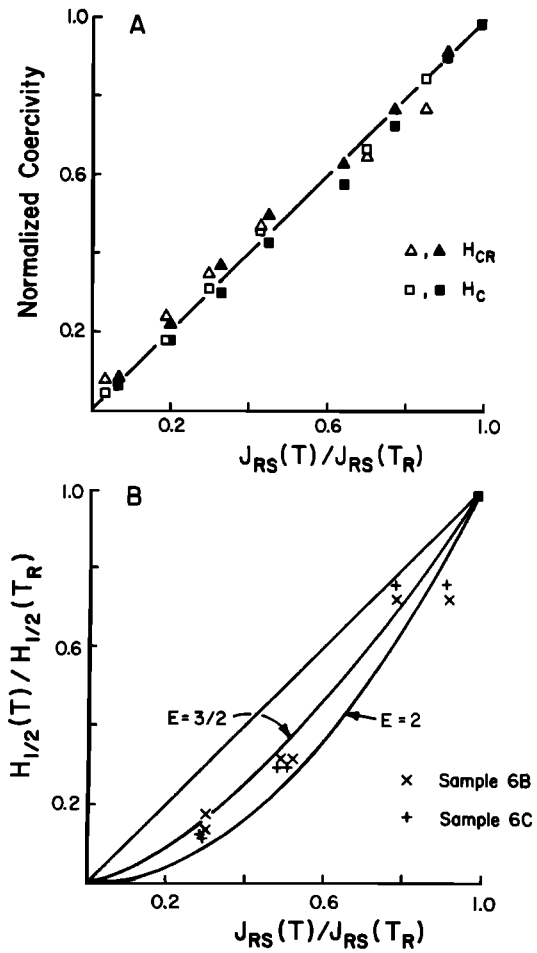

Fig. 7. (*a*) The normalized coercivities H_C (squares) and H_{CR} (triangles) plotted versus the normalized saturation remanence J_{RS} for different temperatures for previously heated CCC magnetite powder. Solid (open) symbols represent undiluted (diluted) powder. Note the linear relation for both H_C and H_{CR}. (*b*) Normalized $H_{1/2}$ values plotted versus normalized J_{RS} for sample 6B (crosses) and sample 6C (pluses), which contain CCC magnetite powder. The curves represent the equation $Y = X^E$, where $X = J_{RS}(T)/J_{RS}(T_R)$; curves are drawn for $E = 1$, $E = \frac{3}{2}$, and $E = \frac{1}{2}$.

cannot go to zero at the Curie temperature, since this would imply a significant change in bond type there, a phenomenon that is well known not to occur. Therefore a reasonable lower limit for J_E is simply J_S itself. We assume in the above that J_E decreases relatively smoothly with temperature. We exclude such hypothetical cases as that in which (1) J_E first increases with temperature above T_R before decreasing and (2) J_E decreases more rapidly than J_S. The limits of A can then be obtained from (6):

$$\left[\frac{J_S(T)}{J_S(T_R)}\right]^3 \leq \frac{A(T)}{A(T_R)} \leq \left[\frac{J_S(T)}{J_S(T_R)}\right]^2 \tag{7}$$

With the usual approximation that the domain wall width (at least at temperatures close to room temperature) is linearly proportional to $(A/K)^{1/2}$ [*Chikazumi*, 1964, p. 191], we use (5) and inequality (7) to find

$$\left[\frac{J_S(T_R)}{J_S(T)}\right]^{5/2} \leq \frac{\delta(T)}{\delta(T_R)} \leq \left[\frac{J_S(T_R)}{J_S(T)}\right]^3 \tag{8}$$

We note that this predicts that a domain wall's thickness approaches infinity close to the Curie temperature, where J_S approaches zero [*Verhoogen*, 1959]; or, considering the geometric limits imposed by grain size, a wall will increase until it fills the grain. This calculation neglects the effects of domain wall shape anisotropy.

The role of shape anisotropy of the domain wall can be approximated by considering a 180° domain wall in which the atomic magnetic moments vary as the sine function from 0° to 180°. The net wall moment is $(2/\pi)J_S$ per unit cross-sectional volume, and it is directed perpendicularly to the moments of the adjacent domains [*Stacey and Banerjee*, 1974, p. 60]. Even though the magnetization is nonuniform, the corresponding shape demagnetization energy probably is reasonably well approximated by $2\Delta N J_S^2/\pi^2$, where ΔN is the difference in the appropriate demagnetizing factors.

Since the magnetocrystalline anisotropy energy decreases much more rapidly than magnetostatic self-energy, a temperature will be reached, defined as the crossover temperature, at which the shape anisotropy becomes dominant. This occurs when $2\Delta N J_S^2/\pi^2 > K$. A crossover temperature is always reached, since K decreases much more rapidly with temperature than J_S^2 (equation (5)). Technically speaking, both shape anisotropy and magnetocrystalline anisotropy energies always contribute to the wall energy; this is particularly true near the crossover temperature. However, to obtain a first-order approximation, we substitute the shape anisotropy for K above the crossover temperature. This yields the following brackets on wall thickness:

$$\left[\frac{J_S(T)}{J_S(T_R)}\right]^{1/2} \leq \frac{\delta(T)}{\delta(T_R)} \leq \left[\frac{J_S(T)}{J_S(T_R)}\right]^0 = 1 \tag{9}$$

Therefore it appears that domain walls monotonically increase in size until a temperature is reached for which shape anisotropy dominates; this results in a decrease in the wall's thickness with further increase in temperature, unless the upper limit is applicable, in which case the wall's thickness is constant.

Possible Interpretations for the Increase in $H_{1/2}$ With Temperature in MD Grains

We begin by considering possible effects associated with changes in domain wall thickness. To do this, we use a simplified model given by *Chikazumi* [1964, pp. 285–287] for calculating the critical field required to move a domain wall over a particular energy barrier. Clearly, one can expect that the larger the critical field required, the larger $H_{1/2}$ will be, all other factors being equal. The barriers are assumed to be caused by a sinusoidal distribution of stress accumulations resulting from crystal imperfections. The stress is assumed to be given by $\sigma = \sigma_0 \cos 2\pi (x/l)$, where σ_0 is its maximum amplitude, x is the displacement coordinate, and l is the wavelength of the stress centers. We assume that the critical field is directly related to $H_{1/2}$ and H_{cl}. One obtains [*Chikazumi*, 1964, p. 286]

$$H_{\text{critic}} = \frac{\pi\lambda\sigma}{J_S \cos\theta}\frac{\delta}{l} \tag{10}$$

where δ is the domain wall thickness, λ is the appropriate magnetostrictive constant, J_S is the saturation magnetization, and θ is the angle between J_S and the applied field. Equation (10) is derived for $l > \delta$. Starting with $l \gg \delta$, we see that H_{critic} will increase with increasing domain wall thickness δ. Because the domain wall width has been shown to increase initially with temperature, the critical field will also increase, provided that the increase in the domain wall width predominates over the temperature variations of the other parameters. A maximum will occur either because δ becomes larger than l, a situation that invalidates the assumptions used to derive (10), because shape anisotropy becomes dominant and the domain wall thickness decreases, or because of the accumulative effect of the temperature variations of λ, σ, and J_S.

An alternative explanation for the maximum in $H_{1/2}$ involves the experimental design. It is important to note that with each increase in temperature in the hot af demagnetization runs one is removing the remanence that was blocked below the peak temperature of the experiment. Let T^* denote any temperature below $T_{\max}$, the temperature at which $H_{1/2}$ is maximum. Then a maximum in $H_{1/2}$ can occur if the remanence blocked below T^* has a lower af demagnetization stability than the remanence blocked above T^*. That is, there is a direct correlation between $H_{1/2}$ and blocking temperature for the TRM blocked below $T_{\max}$. Although our experiments are inadequate to determine which of the above mechanisms is primarily responsible for the observed behavior, in some samples both mechanisms probably contribute to it.

Dependence of Critical Domain Size on External Fields

Introduction

It is well known that many properties of remanent magnetization depend on the field strength used to produce the remanence of the sample. As will be shown here for the first time, it appears that actual critical domain sizes also depend on the field strength.

Calculations to determine critical sizes for the SD–MD transitions are obtained by comparing the magnetic energies of different domain configurations, for example, comparing the SD state with that of a spherical arrangement of the spins (Néel, cited by *Kittel* [1949]; also *Morrish and Yu* [1955]), or by comparing the SD state with a two-domain configuration [*Kittel*, 1949; *Amar*, 1958; *Butler and Banerjee*, 1975] or a four-domain configuration [*Kittel*, 1949; *Stacey*, 1963]. It is postulated in these calculations that the particle will assume the geometry of minimum energy. Although the calculations usually neglect the effects of external fields, it is easy to see that an external field parallel to the magnetization of a SD particle will

tend to increase the critical size for the transition from SD to any of the configurations with inhomogeneous magnetization mentioned above.

The problem is that when one is dealing with remanent magnetization, one is necessarily dealing with a nonequilibrium state. Therefore minimization of energy principles used to calculate critical sizes theoretically and which assume equilibrium conditions is not necessarily applicable.

Experimental Results

The contention that critical domain sizes depend on external fields, which has been suggested by *Dickson et al.* [1966], is supported by data given in Figure 8 showing af demagnetization of TRM acquired in different field strengths for sample 7 (mean particle diameter, 0.21 μm). We see that the relative stability, as measured by af demagnetization, increases with external field strength between 0.10 and 0.25 Oe and decreases with external field strength above 0.49 Oe. (Alternating frequency demagnetization was carried out to 1000 Oe, but the results of af values greater than 500 Oe are difficult to interpret because they are overprinted by ARM. See *Levi* [1974] for further discussion on this point.) On the basis of the Lowrie-Fuller test [*Lowrie and Fuller*, 1971], which distinguishes SD and PSD from MD behavior [*Dunlop et al.*, 1973; *Johnson et al.*, 1975], the remanence in this 0.21-μm-mean-diameter sample behaves as if it were in SD or PSD particles when the TRM is acquired in fields greater than a critical field h_c, where $0.10 < h_c < 0.49$ Oe, and like MD particles for fields less than h_c. It is important to note that additional data strongly support this finding. Data identical to those of sample 7 shown in Figure 8 were also obtained for sample 6A, which contains the same magnetite powder as sample 7. In addition, for a sample from the Olby flow, which is known to contain predominantly SD particles [*Whitney et al.*, 1971], the af stability decreases monotonically with increasing TRM fields. The same TRM fields were used for all three samples, and the heating conditions were identical.

Discussion

The reason for this behavior can be understood by considering a simple example. Suppose the equilibrium configuration for a grain at room temperature and in the absence of an external magnetic field is the two-domain state. Now suppose that we cool this grain in a large magnetic field. If the field is large enough, there will be no domain wall in the grain. Suppose further that the remanence is blocked while the grain is in this uniformly magnetized state. At room temperature, after the field is removed, the grain would like to be in the two-domain state, the equilibrium state. However, to do this, it must nucleate a wall. Because of exchange coupling, this is most easily accomplished at the grain's surface, and the wall must traverse the grain from the boundary to the equilibrium position in the center of the grain. Therefore, there is a net activation energy in going from the SD to the MD state that consists of the nucleating energy for the domain wall and its traverse energy, that energy required for the wall to move from the grain's boundary to its interior. Depending on the particle geometry, defect structures, etc. this energy might be sufficiently great to maintain a nonequilibrium configuration as a metastable state with a very long time constant. Interestingly, in this case the appropriate relaxation time for the remanence might well be that associated with the change in the state of magnetic configuration of the grain.

Using the model of the previous paragraph, we can readily

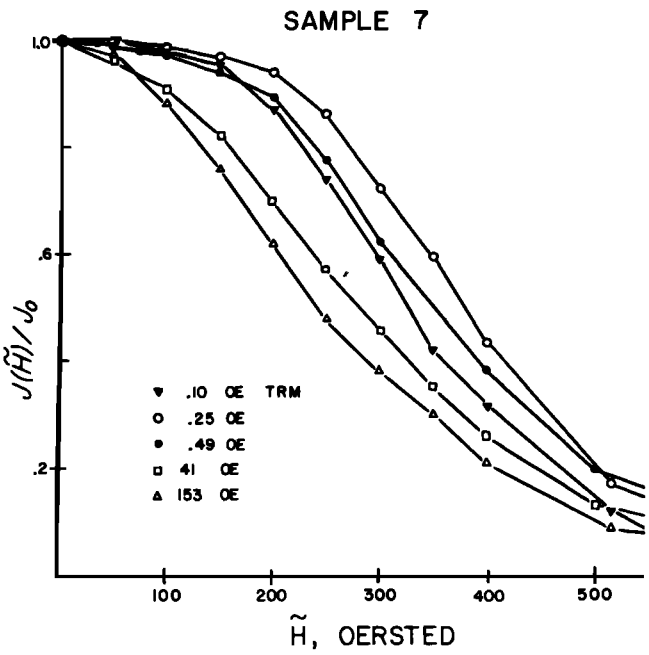

Fig. 8. Stepwise af demagnetization curves of TRM's induced in different magnetic fields in sample 7, which contains equidimensional magnetite particles whose mean diameter is 0.21 μm. Note that the most stable demagnetization curve corresponds to the 0.25-Oe TRM and not to the 0.10-Oe TRM, which is the lowest inducing field used. The 0.49-Oe TRM is also more stable than the 0.10-Oe TRM.

explain the demagnetization curves of Figure 8. We suppose that for TRM-producing fields $h > h_c$ the particles contain no domain walls. If af demagnetization occurs by the nucleation of a domain wall and its subsequent translation, then for $h > h_c$ the stability of these particles should exceed that of truly MD particles, whose af demagnetization is by domain wall movements only. Although the required energy for wall nucleation is not known, it seems reasonable that the af stability of such submicron particles would be less than that for true SD particles (sample 11, Table 3), whose demagnetization is by the rigid rotation of the magnetic moments. Because the observational data are indirect, it is possible that for $h > h_c$, demagnetization might occur by a mode of nonrigid rotation of the magnetic moment, such as magnetization curling [*Frei et al.*, 1957]. Similar to the explanation of *Lowrie and Fuller* [1971] for SD particles is the expectation that for $h > h_c$ the af stability would decrease with increasing TRM fields. For $h < h_c$ the particles are supposed to contain a domain wall, af demagnetization is by domain wall movements, and the af stability is expected to increase with increasing TRM fields [*Lowrie and Fuller*, 1971]. However, even for $h < h_c$ the af stability of these submicron PSD particles should be substantially greater than it is for bulk MD material because of the particles' small size and the relatively large interaction between the domain walls and the crystal surfaces.

For the CCC magnetite powder at room temperature, $J_{RS}/J_S = 0.12$ (Table 1), which is substantially less than the 0.50 value expected for a random distribution of SD particles. This condition could be due, in part, to the presence of MD and superparamagnetic particles in the assemblage, but it might also be due to particles which, though they are not MD in the classical sense, are inhomogeneously magnetized. Such inhomogeneous magnetization might be caused by shape demagnetizing effects of the particles' crystal surfaces.

The Lowrie-Fuller test has become a very popular tool for

distinguishing the domain state of magnetic particles. *Johnson et al.* [1975] used ARM in studying the biasing-field dependence of af demagnetization characteristics. They found SD Lowrie-Fuller behavior of equidimensional particles of diameters of 0.2 μm. Thus they conclude that either the SD–PSD transition occurs at a diameter greater than 0.2 μm or the Lowrie-Fuller test does not distinguish between SD and PSD particles. The submicron magnetite particles used by *Johnson et al.* [1975] were prepared by precipitation from an aqueous solution, and they were substantially oxidized. *Bailey* [1975] also used ARM and observed a gradual change from SD to MD type Lowrie-Fuller behavior between 2 and 15 μm, suggesting that the PSD-MD boundary is at least several micrometers. Bailey's magnetite particles were obtained by grinding down larger particles, and the particles were not annealed prior to the af demagnetization experiments. *Dunlop* [1973], using both TRM and ARM, obtained SD characteristics of the Lowrie-Fuller test for submicron magnetite particles. Rarely, however, are the TRM-producing fields less than 1 Oe. The estimate of *Bailey and Dunlop* [1975] is consistent with recent experiments of *Day et al.* [1976], who defined MD behavior to be when $H_{CR}/H_C > 3$ and $J_{RS}/J_S \lesssim 0.05$. Day et al. suggest that the PSD–MD transition occurs between 10 and 20 μm.

Some of these differences in critical size estimates are undoubtedly the result of variations in the size of the inducing field. Figure 8 shows that for $h > 0.50$ Oe, SD behavior is obtained for sample 7, which has a mean particle diameter of 0.21 μm. Yet for fields less than h_c, MD behavior is exhibited. Differences in estimates of critical size can result from the size of the inducing field, variations in shape anisotropy, variations in chemistry, variations in internal stress, and the use of different types of remanence. Although we are somewhat surprised that such variations can produce such large differences in critical size estimates, variations in the TRM-producing field strength appear to provide the most plausible explanation for our experimental results.

It appears that numerous subtle factors, including field strength, can greatly affect estimates of SD-PSD and PSD-MD critical sizes. Because these factors are undoubtedly present in natural situations, one should expect a wide range of critical sizes in rocks.

Conclusions

In this paper we have measured numerous properties of SD, PSD, and MD grains. We have found that the stability with respect to low-temperature cycles to below magnetite's isotropic temperature is the most consistent indicator for domain structure in magnetite: minimum stability for large MD particles, increasing stability with decreasing particle size, and maximum stability for acicular SD particles. This behavior is consistent with the diminishing role of magnetocrystalline anisotropy with decreasing particle sizes and a corresponding enhancement of shape anisotropy in controlling the remanence. Although the amount of remanence loss during a low-temperature cycle does not depend simply on grain volume but on other factors such as internal stress [*Merrill*, 1970], low-temperature cycles appear to be of great aid in determining whether a magnetite sample primarily consists of SD, PSD, or MD particles. In our studies the decrease of TRM (or ARM) in SD particles due to low-temperature cycles is typically less than 2 or 3%; in submicron particles that are larger than SD size, it is in the range of 5–20%, while in large MD particles it is greater than 50%.

The stability with respect to thermal demagnetization is the least faithful stability indicator for predicting domain structure in magnetite because some MD remanence is blocked at high temperatures in excess of 500°C.

At room temperature, af demagnetization remains the most effective demagnetization procedure for assuring that the remaining remanence is in submicron grains.

We have shown that a typical domain wall width increases with temperature until a crossover temperature is reached. Above the crossover temperature the shape anisotropy energy of a domain wall dominates the magnetocrystalline anisotropy energy. This result possibly explains why the temperature dependence of $H_{1/2}$ exhibits a broad maximum for MD particles. On the other hand, the $H_{1/2}$ versus T curves for the SD and PSD samples are similar to one another, decreasing linearly with temperature between T_R and 500°C. The similarity of the curves suggests that the same anisotropy is responsible for the TRM of these PSD and SD samples.

It is well recognized that critical sizes for transitions between SD, PSD, and MD behavior depend on grain shape and temperature (for example, see *Butler and Banerjee* [1975]). In addition, we have shown that several other factors can affect critical size estimates, such as the type of remanence involved and the strength of the field used in the experiments. Because of this and because activation energy is required to pass from one magnetic configuration to another, it is possible that a remanence at room temperature resides in grains that are not in their equilibrium configuration. The appropriate relaxation time of an ensemble of such grains may be very different from that previously assumed. Finally, this work clearly demonstrates that the various criteria used to estimate critical sizes (Lowrie-Fuller test, hysteresis parameter analyses, low-temperature treatments, etc.) can give inconsistent results. This comes about because the different methods used either are dealing with different types of remanence or involve experiments conducted at different temperatures, where the magnetic parameters are different.

Notation

- J_S saturation magnetization, the magnetization measured in the presence of a saturating field.
- J_{RS} saturation remanence, the remanence after the saturating field has been removed.
- H_{ci} microscopic or intrinsic coercivity of a magnetic particle.
- H_C bulk coercivity, the coercivity which refers to the reversed field required to reduce to zero the net sample magnetization, after the sample has been magnetized to saturation.
- H_{CR} remanence coercivity, the magnitude of the reversed field required so that when this reversed field is reduced to zero, the sample is left with zero magnetization.
- $H_{1/2}$ median destructive field, the peak alternating field required to reduce the remanence to half its initial value.
- T temperature in degrees Celsius or degrees Kelvin; T_C is the Curie point; T_R is room temperature; T_B is blocking temperature.
- $\langle T_B \rangle$ median blocking temperature of the sample, the temperature to which the sample must be heated in zero field so that its remanence at T_R equals one-half its initial value.

Acknowledgments. Comments or preprints from D. Dunlop, M. Bailey, R. Day, M. Fuller, V. Schmidt, and P. Shive were very helpful. Funding for this research was provided by the National Science Foundation (GA-40496 and OCE 75-21002) and the National Aeronautics

and Space Administration (NGR 24-005-248). Contribution 972 of the Department of Oceanography, University of Washington, Seattle.

REFERENCES

Amar, H., On the width and energy of domain walls in small multidomain particles, *J. Appl. Phys., 28,* 732–733, 1957.

Amar, H., Magnetization mechanism and domain structure of multidomain particles, *Phys. Rev., 111,* 149–153, 1958.

Bailey, M. E., The magnetic properties of pseudosingle domain grains, M.S. thesis, 71 pp., Univ. of Toronto, Toronto, Ont., Canada, 1975.

Bailey, M. E., and D. J. Dunlop, Preisach analysis of pseudo-single domain magnetite and a rationale for the 'Lowrie-Fuller' test (abstract), *Eos Trans. AGU, 56,* 975, 1975.

Butler, R. F., and S. K. Banerjee, Theoretical single-domain grain size range in magnetite and titanomagnetite, *J. Geophys. Res., 80,* 4049–4058, 1975.

Chikazumi, S., *Physics of Magnetism,* 554 pp., John Wiley, New York, 1964.

Cullity, B. D., *Introduction to Magnetic Materials,* 666 pp., Addison-Wesley, Reading, Mass., 1972.

Davis, P. M., and M. E. Evans, Interacting single-domain properties of magnetite intergrowth, *J. Geophys. Res., 81,* 989–994, 1976.

Day, R., M. Fuller, and V. A. Schmidt, Magnetic hysteresis properties of synthetic titanomagnetites, *J. Geophys. Res., 81,* 873–880, 1976.

Dickson, G. O., C. W. F. Everitt, L. G. Parry, and F. D. Stacey, Origin of thermoremanent magnetization, *Earth Planet. Sci. Lett., 1,* 222–224, 1966.

Dunlop, D. J., Hysteretic properties of synthetic and natural monodomain grains, *Phil. Mag., 19,* 329–338, 1969.

Dunlop, D. J., Magnetite: Behavior near the single-domain threshold, *Science, 176,* 41–43, 1972.

Dunlop, D. J., Thermoremanent magnetization in submicroscopic magnetite, *J. Geophys. Res., 78,* 7602–7613, 1973.

Dunlop, D. J., and M. Bina, The coercive force spectrum of magnetite at high temperatures: Evidence for thermal activations below the blocking temperature, submitted to *Geophys. J.,* 1977.

Dunlop, D. J., and G. F. West, An experimental evaluation of single-domain theories, *Rev. Geophys. Space Phys., 7,* 709–757, 1969.

Dunlop, D. J., J. A. Hanes, and K. L. Buchan, Indices of multidomain magnetic behavior in basic igneous rocks: Alternating field demagnetization, hysteresis, and oxide petrology, *J. Geophys. Res., 78,* 1387–1393, 1973.

Dunlop, D. J., F. D. Stacey, and D. E. W. Gillingham, The origin of thermoremanent magnetization: Contribution of pseudo-single domain magnetic moments, *Earth Planet. Sci. Lett., 21,* 288–294, 1974.

Elmore, W. C., Ferromagnetic colloid for studying magnetic structures, *Phys. Rev., 54,* 309–310, 1938.

Evans, M. E. and M. L. Wayman, An investigation of small magnetic particles by means of electron microscopy, *Earth Planet. Sci. Lett., 9,* 365–370, 1970.

Evans, M. E., M. W. McElhinny, and A. C. Gifford, Single-domain magnetite and high coercivities in a gabbroic intrusion, *Earth Planet. Sci. Lett., 4,* 142–146, 1968.

Everitt, C. W. F., Thermoremanent magnetization, I, Experiments on single domain grains, *Phil. Mag., 6,* 713–726, 1961.

Everitt, C. W. F., Thermoremanent magnetization, II, Experiments on multidomain grains, *Phil. Mag., 7,* 583–597, 1962*a*.

Everitt, C. W. F., Thermoremanent magnetization, III, Theory of multidomain grains, *Phil. Mag., 7,* 599–616, 1962*b*.

Fletcher, E. J., Ph.D. thesis, Univ. of Newcastle upon Tyne, Newcastle upon Tyne, England, 1971.

Frei, E. H., S. Shtrickman, and D. Treves, Critical size and nucleation field of ideal ferromagnetic particles, *Phys. Rev., 106,* 446–455, 1957.

Gallagher, K. J., W. Feitknecht, and U. Mannweiler, Mechanism of oxidation of magnetite to γFe_2O_3, *Nature, 217,* 1118–1121, 1968.

Hargraves, R. B., and W. M. Young, Source of stable remanent magnetization in Lambertville diabase, *Amer. J. Sci., 267,* 1161–1177, 1969.

Hoblitt, R. P., and E. E. Larson, New combination of techniques for determination of the ultrafine structure of magnetic minerals, *Geology,* 723–726, 1975.

Johnson, H. P., and R. T. Merrill, Magnetic and mineralogical changes associated with low-temperature oxidation of magnetite, *J. Geophys. Res., 77,* 334–341, 1972.

Johnson, H. P., W. Lowrie, and D. V. Kent, Stability of anhysteretic remanent magnetization in fine and coarse magnetite and maghemite particles, *Geophys. J. Roy. Astron. Soc., 41,* 1–10, 1975.

Kittel, C., Physical theory of ferromagnetic domains, *Rev. Mod. Phys., 21,* 541–583, 1949.

Klapel, G. D., and P. N. Shive, High-temperature magnetostriction of magnetite, *J. Geophys. Res., 79,* 2629–2633, 1974.

Kobayashi, K., and M. D. Fuller, Stable remanence and memory of multidomain materials with special reference to magnetite, *Phil. Mag., 18,* 601–624, 1968.

Kobayashi, K., M. F. Campbell, and J. B. Moorehead, Size dependence of low-temperature change in remanent magnetization of Fe_3O_4, in *Annual Proceedings of the Rock Magnetism Research Group,* pp. 33–50, Tokyo, Japan, 1965.

Levi, S., Some magnetic properties of magnetite as a function of grain size and their implications for paleomagnetism, Ph.D. thesis, 210 pp., Univ. of Wash., Seattle, 1974.

Levi, S., and R. T. Merrill, A comparison of ARM and TRM in magnetite, *Earth Planet. Sci. Lett., 32,* 171–184, 1976.

Lowrie, W., and M. Fuller, On the alternating field demagnetization characteristics of multidomain thermoremanent magnetization magnetite, *J. Geophys. Res., 76,* 6339–6349, 1971.

McElhinny, M. W., *Paleomagnetism and Plate Tectonics,* 358 pp., Cambridge University Press, New York, 1973.

Merrill, R. T., Low-temperature treatments of magnetite and magnetite-bearing rocks, *J. Geophys. Res., 75,* 3343–3349, 1970.

Merrill, R. T., Magnetic effects associated with chemical changes in igneous rocks, *Geophys. Surv., 2,* 277–311, 1975.

Morrish, A. H., *The Physical Principles of Magnetism,* 680 pp., John Wiley, New York, 1965.

Morrish, A. H., and L. A. K. Watt, Coercive force of iron oxide micropowders at low temperatures, *J. Appl. Phys., 29,* 1029–1033, 1958.

Morrish, A. H., and S. P. Yu, Dependence of the coercive force on the density of some iron oxide powders, *J. Appl. Phys., 26,* 1049–1055, 1955.

Néel, L., Théorie du traînage magnétique des ferromagnétiques en grains fins avec applications aux terres cuites, *Ann. Geophys., 5,* 99–136, 1949.

Néel, L., Some theoretical aspects of rock magnetism, *Advan. Phys., 4,* 191–242, 1955.

Ozima, M., and M. Ozima, Origin of thermoremanent magnetization, *J. Geophys. Res., 70,* 1363–1369, 1965.

Ozima, M., M. Ozima, and S. Akimoto, Low temperature characteristics of remanent magnetization of magnetite, *J. Geomagn. Geoelec., 16,* 165–177, 1964.

Parry, L. G., Magnetic properties of dispersed magnetite powders, *Phil. Mag., 11,* 303–312, 1965.

Rahman, A. A., A. D. Duncan, and L. G. Parry, Magnetization of multidomain magnetite particles, *Riv. Ital. Geofis., 22,* 259–266, 1973.

Rathenau, G. W., Saturation and magnetization of hexagonal iron oxide compounds, *Rev. Mod. Phys., 25,* 297–301, 1953.

Schmidt, V. A., A multidomain model of thermoremanence, *Earth Planet. Sci. Lett., 20,* 440–446, 1973.

Soffel, H., The single domain–multidomain transition in natural intermediate titanomagnetites, *Z. Geophys., 37,* 451–470, 1971.

Stacey, F. D., Thermo-remanent magnetization of multidomain grains in igneous rocks, *Phil. Mag., 3,* 1391–1401, 1958.

Stacey, F. D., A generalized theory of thermoremanence, covering the transition from single domain to multi-domain magnetic grains, *Phil. Mag., 7,* 1887–1900, 1962.

Stacey, F. D., The physical theory of rock magnetism, *Advan. Phys., 12,* 45–133, 1963.

Stacey, F. D., and S. K. Banerjee, *The Physical Principles of Rock Magnetism,* 195 pp., Elsevier, New York, 1974.

Strangway, D. W., E. E. Larson, and M. Goldstein, A possible cause of high stability in volcanic rocks, *J. Geophys. Res., 73,* 3787–3795, 1968.

Verhoogen, J., The origin of thermoremanent magnetization, *J. Geophys. Res., 64,* 2441–2449, 1959.

Whitney, J., H. P. Johnson, S. Levi, and B. W. Evans, Investigations of some magnetic and mineralogical properties of the Laschamp and Olby flows, France, *Quaternary Res., 1,* 511–521, 1971.

(Received July 1, 1976;
revised June 24, 1977;
accepted June 29, 1977.)